

APPLICATIONS OF INELASTIC SPD METHOD FOR ESTIMATING RELATIVE DISPLACEMENT TO AVOID POUNDING OF ADJACENT BUILDINGS

B. T. Tran¹⁾ and K. Kasai²⁾

1) Graduate Student, Department of Built Environment, Tokyo Institute of Technology, Japan

2) Professor, Structural Engineering Research Center, Tokyo Institute of Technology, Japan
tthbinh@enveng.titech.ac.jp, kasai@serc.titech.ac.jp

Abstract: Pounding between closely spaced structures can be a serious hazard in seismically active metropolitan areas. Peak relative displacement between these structures can be obtained by the proposed spectral difference (SPD) rule. Unlike time history analysis method, a closed form solution can be applied to discuss trends of relative displacement of buildings in terms of periods, damping ratios, yield strength, ductility demands of the buildings as well as earthquake spectrum. In this study, practical implementation of the SPD rule through a simple procedure is proposed in order to estimate required separation to preclude pounding between adjacent structures. Validation study is conducted, using a relatively large ensemble of 33 ground motion records on a number of various adjacent building pairs that are consistent with the current code requirements for strength and stiffness. Inconsistencies of other spectrum methods and the accuracy of SPD-based method are explained through comparisons with the time history analysis results.

1. INTRODUCTION

In recent years, there has been an increased awareness of the potential impact of buildings during moderate to strong earthquakes due to insufficient separation distance (Bertero 1986, Rosenblueth and Meli 1986, Kasai and Maison 1997). Controlling the relative displacement between adjacent buildings (Fig. 1) is an important method for preventing these buildings pound each other during seismic excitation. The magnitude of the required seismic gap s_{req} can be estimated by calculating their peak relative displacement through time history analysis. However, since one cannot determine specifically the future earthquake time history, a spectrum approach that uses an ensemble from the past as well as potential earthquakes would be more reliable and preferred.

In fact, the peak relative displacement depends not only on the peak displacement of each separate structure but also on the *vibration phase*, which is associated with their elastic and inelastic responses. Therefore, the key parameters such as adjacent building's vibration periods, damping ratios, heights, ductility demands, and even hysteresis types must be taken into account for determining reasonable gap between structures. Kasai et al. (1996) presented a method called "spectral difference (SPD) rule" using response spectrum to estimate the maximum relative displacement. The method provides a closed-form solution that relates those key parameters with the buildings' relative motion. However, using directly this SPD rule requires either inelastic response spectrum or time history analysis to obtain peak inelastic displacement of each separate building.

This study is to propose a practical SPD-based method by implementing more simplifications. The proposed method employs only elastic response spectrum to approximate peak inelastic displacement of each structure. Then it considers a number of various adjacent building pairs having stiffness and strength consistent with the Japanese seismic code and an ensemble of 33 earthquakes scaled to

different levels for the validation study. The accuracy of the SPD-based method is illustrated by comparing results with time history analysis and other methods. We also clarify the trend of the peak relative displacement by explaining the complex effect of the mentioned key factors through this SPD-based method. This work aims to emphasize on the significant effect of yielding on building's phase motion and relative displacement. The study would be useful for understanding and controlling the relative displacement of adjacent structures.

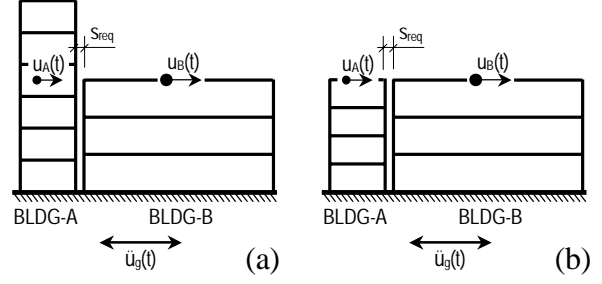


Figure 1. Relative Displacement of Adjacent Bldgs.

2. RELATIVE DISPLACEMENT AND VARIOUS ESTIMATES

2.1 Past Rules

From Fig. 1, the relative displacement $u_{rel}(t)$ between buildings A and B is $u_{rel}(t) = u_A(t) - u_B(t)$, where $u_A(t)$, $u_B(t)$ = displacement time histories at potential pounding locations. From now on, the subscripts ‘‘A’’ and ‘‘B’’ shall refer to buildings A and B, respectively.

Required separation between buildings A and B can be determined as $u_{rel}(TH) = \max |u_{rel}(t)|$, ‘‘TH’’ indicates results from time history analysis, and pounding is avoided if the separation distance $s_{req} > u_{rel}(TH)$.

Two other methods for estimating the peak relative displacement are the absolute-sum (ABS) rule: $u_{rel}(ABS) = u_A + u_B$ and the square-root-of-sum-of-squares (SRSS) rule: $u_{rel}(SRSS) = \sqrt{u_A^2 + u_B^2}$, where u_A , u_B = the absolute peak displacements of the buildings, which can be obtained from the response spectrum. The use of the SRSS rule is stipulated in the U.S. seismic code (IBC, 2000).

2.2 Spectral Difference (SPD) Rule

Unlike the ABS and SRSS rules, the SPD rule (Kasai et al. 1996) uses a cross correlation coefficient ρ_{AB} , and

$$u_{rel}(SPD) = \sqrt{u_A^2 + u_B^2 - 2\rho_{AB}u_Au_B} \quad (1)$$

The ρ_{AB} reflects vibration phase of buildings A and B, and it was derived from a random vibration theory as follows (Kasai et al. 1996, Der Kiureghian 1980):

$$\rho_{AB} = \frac{8\sqrt{\xi_A^*\xi_B^*}(\xi_B^* + \beta^*\xi_A^*)\beta^{*1.5}}{(1 - \beta^{*2})^2 + 4\xi_A^*\xi_B^*(1 + \beta^{*2})\beta^* + 4(\xi_B^{*2} + \xi_A^{*2})\beta^{*2}} \quad (2)$$

where β^* = ratio of effective vibration periods T_B^*/T_A^* , ξ_A^* and ξ_B^* = effective damping ratios. Note that $0 \leq \rho_{AB} \leq 1$, and larger ρ_{AB} means more in-phase motion, and consequently smaller u_{rel} (Eq. 1).

Eq. 2 explains that T^* and ξ^* play a key role in vibration phase. When β^* is close to 1, and/or ξ_A^* and ξ_B^* are large, ρ_{AB} approaches 1, and in-phase motion develops. Inclusion of damping comes from the fact that damping tends to eliminate a free vibration portion of the seismic response, and mainly a forced vibration portion remains, making the two buildings vibrate similarly to the

ground motion (Kasai et al., 1996; Kasai et al., 2002).

For the buildings of bilinear hysteresis (Fig. 2a) and stiffness degrading hysteresis (Fig. 2b), the above effective properties are given as:

$$\text{Bilinear:} \quad T^* = T[1 + 0.09(\mu - 1)] \quad ; \quad \xi^* = \xi + 0.084(\mu - 1)^{1.3} \quad (3a)$$

$$\text{Degrading:} \quad T^* = T[1 + 0.18(\mu - 1)] \quad ; \quad \xi^* = \xi + 0.16(\mu - 1)^{0.9} \quad (3b)$$

where T , ξ , μ = initial elastic vibration period, initial viscous damping ratio, and peak ductility demand, respectively.

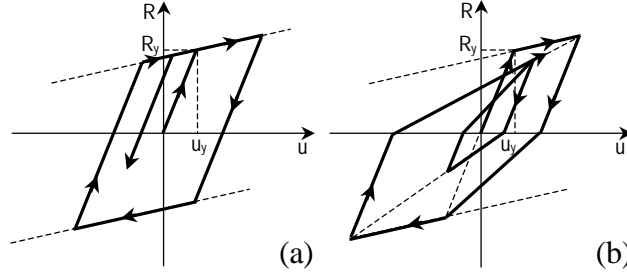


Figure 2. Hysteresis Behavior: (a) Bilinear Building Model, and (b) Stiffness Degrading Model.

3. TRENDS OF RELATIVE MOTION AND PHASE

3.1 Trends of Relative Motion

Consider two single-degree-of-freedom (SDOF) systems A and B with initial vibration periods T_A and $T_B = 1.0s, 1.3s$, and initial viscous damping ratios $\xi_A = \xi_B = 0.02$. The stiffness degrading hysteresis model (Fig. 2b) is used with strain-hardening ratio 5%. The system is designed under the three cases described below, and they are subjected to the 1940 Imperial Valley earthquake (117 El Centro station, 0.35g).

Case 1: Systems are elastic and only small damping is given. Thus, they must vibrate mostly out-of-phase.

Case 2: Systems are inelastic and designed to develop $\mu_A = \mu_B = 3$. In-phase motion is promoted due to the hysteretic damping.

Case 3: Systems are inelastic, and designed to develop distinct values of $\mu_A = 6$ and $\mu_B = 3$. Like case 2, in-phase motion develops due to hysteretic damping. In addition, although $T_B/T_A = 1.3$, different μ_A and μ_B causes $T_B^*/T_A^* \approx 1$, may lead to strong in-phase motion.

As Fig. 3a shows, Case 1 develops out-of-phase movement between the elastic systems A and B due to their different periods. In contrast, the responses of inelastic systems in Cases 2 and 3 are significantly in phase (Figs. 3b, and 3c). Fig. 3d plots $u_{rel}(t)/(u_A + u_B)$, which highlights increasing trend of the in-phase motion in the order of Cases 1, 2, and 3. Table 1 lists magnitudes of each response quantity.

The SPD, SRSS, and ABS rules are used to estimate u_{rel} of the above three cases by using the peak displacements u_A, u_B obtained from the time history analyses. In case of the SPD method, the values are also divided by the yield displacements to calculate μ_A, μ_B , and the cross correlation ρ_{AB} (Eq. 2)

Table 2 indicates superior prediction of u_{rel} by the SPD rule. The errors of the SRSS and ABS rules increase, especially when buildings exhibit large inelastic deformations. Eqs. 1 to 3 of the SPD rule, therefore, could clarify the complex effects from the initial vibration periods, viscous damping ratios, and ductility demands varied herein. This point will be further demonstrated below.

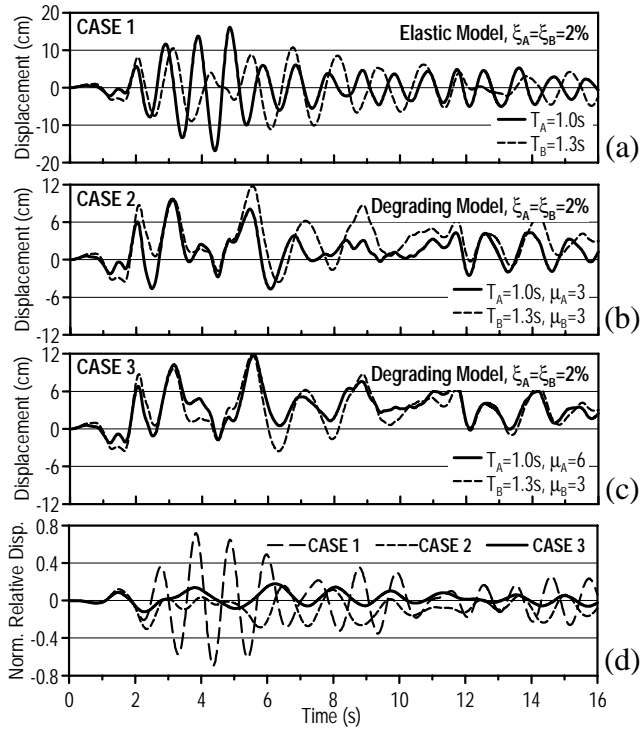


Figure 3. Time History Responses of the Systems in Three Cases.

3.2 Trends of Vibration Phase

Fig. 4 beside plots cross correlation coefficients ρ_{AB} (Eq. 2) in order to illustrate general trends of systems' phase. For elastic systems (Fig. 4a), the ρ_{AB} is high only if both $T_B/T_A \approx 1$ and $\xi_B/\xi_A \approx 1$, and it is very low otherwise. For inelastic systems, however, $T_B/T_A \neq 1$ can lead to the largest ρ_{AB} , depending on the values of μ_A and μ_B (Figs. 4c and 4d). This is because the effective period and damping, instead of initial period and damping, governs ρ_{AB} when systems are inelastic. Case 3 gives a typical example, where $T_B^*/T_A^* \approx 0.93$ (Table 2) in contrast to $T_B/T_A = 1.3$, and it gave the smallest u_{rel} among all cases (Fig. 3).

Since T^* and ξ^* are affected by the ductility demand μ , Fig. 4 provides the direct and useful information regarding the effect of μ . The peaks of the ρ_{AB} -curves are close to 1.0 for a wide range of T_B/T_A when $\mu > 2$, indicating importance of including even moderate amount of yielding.

Thus, large ρ_{AB} results even when the initial period ratio $T_B/T_A \neq 1$, and maximum ρ_{AB} is obtained when systems A and B have different μ 's. This is the reason why Case 3 shows more in-phase motion than Case 2.

Table 1. Results of Three Considering Cases.

Case	Ductility		Peak Disp. (cm)			$\frac{u_{rel}}{\max(u_A, u_B)}$	$\frac{u_{rel}}{u_A + u_B}$
	μ_A	μ_B	u_A	u_B	u_{rel}		
1	1	1	16.81	11.09	20.02	1.19	0.72
2	3	3	9.70	11.77	6.50	0.55	0.30
3	5	3	11.84	11.77	4.23	0.57	0.18

Table 2. Approximation Results Using SPD and Other Methods.

Case	Effective Parameters				ρ_{AB}	$\frac{u_{rel}(SPD)}{u_{rel}(TH)}$	$\frac{u_{rel}(SRSS)}{u_{rel}(TH)}$	$\frac{u_{rel}(ABS)}{u_{rel}(TH)}$
	T_A^*	T_B^*	ξ_A^*	ξ_B^*				
1	1.00	1.30	0.02	0.02	0.02	1.00	1.01	1.39
2	1.36	1.77	0.32	0.32	0.85	0.96	2.35	3.30
3	1.90	1.77	0.70	0.32	0.91	1.19	3.95	5.58

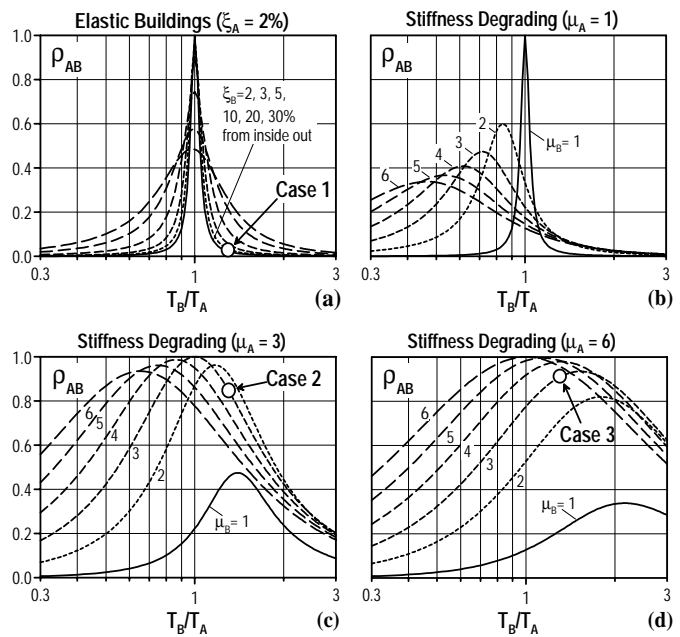


Figure 4. General Trends of Buildings' Phase.

4. SIMPLIFIED SPD-BASED METHOD

4.1 Inelastic Displacement Prediction by Elastic Spectrum

Studies have been conducted worldwide to predict inelastic response via elastic spectrum. They utilize the strong correlation between the ductility demand μ and the strength reduction factor R_μ .

$$R_\mu = \frac{Q_e}{Q_y} = \frac{\Delta_e}{\Delta_y} \quad (4)$$

where Q_y, Δ_y = yield shear and yield displacement of the system given, and Q_e, Δ_e = base shear and displacement when the system is presumed to behave elastically. The above displacements are defined at the effective height (Chopra 1995) H_{eff} of the building.

The μ - R_μ relationships have been proposed by Newmark and Hall (1973), Uang (1992), and others. In the present study, we will utilize Nassar and Krawinkler's rule (1991) as follows:

$$\mu = 1 + \frac{R_\mu^c - 1}{c} \quad ; \quad c = \frac{T^a}{1 + T^a} + \frac{b}{T} \quad (5a,b)$$

where a and b depend on the strain-hardening ratio α .

Once Δ_e is estimated from an elastic spectrum, μ is obtained from Eqs. 4 and 5, and the peak inelastic displacement Δ at height H_{eff} is

$$\Delta = \mu \cdot \Delta_y \quad (6)$$

Following Nassar and Krawinkler (1991), Uang (1992), and Kasai et al. (2003), the damping ratio shall be 5% when using the elastic spectrum.

4.2 Step-by-Step Procedure for Simplified SPD-Based Method

For simplified prediction of u_{rel} without conducting time history analysis, we combine the SPD rule with elastic response spectrum. The height of building A is set equal to or greater than that of building B, i.e., $H_A \geq H_B$ will be considered (Fig. 1).

The procedure obtains the following parameters in order:

- (1) Elastic displacements Δ_{eA} and Δ_{eB} from elastic spectrum.
- (2) Inelastic displacements Δ_A and Δ_B using Eqs. 4 to 6.
- (3) Inelastic displacements u_A and u_B at the common critical height.
- (4) Effective periods T_A^* and T_B^* , damping ratio ξ_A^* and ξ_B^* from Eqs. 3.
- (5) Cross correlation ρ_{AB} from Eq. 2, and $s_{req} = u_{rel}(SPD)$ from Eq. 1.

In the present study, a simple straight-line building deformation mode is assumed. For step (3) above, therefore, effective height $H_{eff} = 2H/3$ is considered for each building, and the following relationship is used: $u_A = 1.5(H_B/H_A) \Delta_A$, and $u_B = 1.5 \Delta_B$

4.3 Building Models Consistent with Code

Building models to be used in the following sections will be defined here. The preliminary data required for the application of the SPD-based method are the initial period T and the yield displacement Δ_y of each building. From now on, T is assumed to coincide with that given by the Japanese Seismic Code (IAEE, 1996), i.e., $T = 0.03H$ and $T = 0.02H$, where H = total height of the building in meters, for steel building and concrete building, respectively.

Building yield shear is set to $\Omega \cdot Q_y$, where Ω = overstrength factor, and Q_y = yield shear required by the code such as:

$$Q_y = C_0 \cdot R_t \cdot W \quad (7)$$

In Eq. 7, $C_0 = 0.25$ and 0.30 are assumed for the steel and concrete buildings, respectively. The values are somewhat arbitrary as long as $C_0 \geq 0.2$, and they are made equal to the D_s -factors (IAEE, 1996). Indeed, these higher values may better approximate the actual behavior. However, note also that the overstrength factor Ω can be varied, making the specific C_0 -value less significant.

The design spectral coefficient R_t is obtained from the formula as specified in Japanese Seismic Code (IAEE, 1996), where medium soil can be assumed. Based on these, the yield displacement Δ_y at height H_{eff} is calculated as:

$$\Delta_y = C_0 \cdot R_t \cdot g (T/2\pi)^2 \quad (8)$$

5. VALIDATION OF SIMPLIFIED SPD-BASED METHOD

5.1 Parameters Considered for Validation

A validation study is now conducted in order to examine the accuracy of the SPD-based method, and to obtain the general trend of u_{rel} between the building pairs consisting of various steel and concrete frames. In this study, buildings have 8 different heights of 3, 6, 9, 12, 15, 18, 21, and 24 stories with a common story height of 4m. For building pairs A and B, all possible combinations of 8 different heights are considered with the condition of $H_A \geq H_B$ (Fig. 1). The total number of building pairs is 36.

Additionally, 4 cases of material type combinations for buildings A and B are assumed: steel vs. steel; concrete vs. concrete; steel vs. concrete; and concrete vs. steel, respectively. In total, the number of building pairs is 144 [(36 height combinations) x (4 material type combinations)].

For each building pair, 31 past earthquakes and 2 artificial earthquakes (Kasai et al. 2003) are used, and each record is applied in both positive and negative directions. The records cover a variety of seismic intensities, and it is reasonable to scale them to the same peak ground acceleration (PGA). Thus, 4 different PGA scales of 0.2g, 0.4g, 0.6g, and 0.8g are considered for each record. In total, the number of earthquakes considered for each building pair is 264 [(33 earthquakes) x (2 directions) x (4 PGA scales)].

Fig. 5 shows the mean acceleration spectrum and mean \pm standard deviation of 33 records scaled to 0.4g. Fig. 5 also shows $R_t \cdot g$ curve for the medium soil condition. Yield strengths of 8 steel buildings and 8 concrete buildings are also plotted, respectively.

Using the elastic spectrum of each earthquake, inelastic peak displacement is estimated, and used for all the SPD-, SRSS-, and ABS-based methods. Also, in order to obtain exact solution for u_{rel} , dynamic time history analyses are conducted using a SDOF nonlinear analysis program NONSPEC (Mahin and Lin 1983). In summary, this validation study examines a total of 38,016 cases [(144 building pairs) x (264 scaled records)].

5.2 Validation Results

For each of the cases mentioned above, the ratios of $u_{rel}(\text{SPD})$, $u_{rel}(\text{SRSS})$, and $u_{rel}(\text{ABS})$ to the

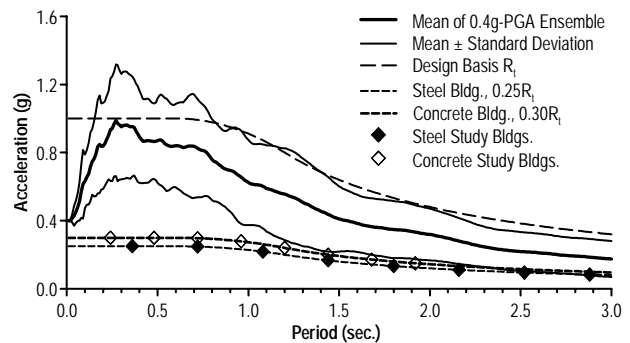


Figure 5. Mean and Deviation of 33 Acceleration Spectra (PGA=0.4g), Design Spectrum and Design Strength of Buildings.

$u_{rel}(TH)$ are obtained, and they are averaged over 36 height combinations and 2 earthquake directions per combination of material type, earthquake, and PGA scale. The average values are shown in Fig. 6.

Fig. 6 shows that $u_{rel}(SPD)/u_{rel}(TH) \approx 1$ for most cases, indicating superior accuracy of the SPD-based method. ABS- or SRSS-based method appears to be largely conservative, as the PGA scale increases. This is because they do not account for the important effect of inelastic deformation, which, under stronger earthquake causes more in-phase motion between the two buildings.

The important effect of inelastic in-phase motion is seen especially for the strong earthquakes like Kobe Japan (earthquakes 7 to 12), Iran and Northridge (earthquakes 17 to 22). These earthquakes, even scaled to the same PGA as other earthquakes, force each building to deform larger due to their higher spectral values over a wide period range, but they also produce at the same time more in-phase motion between the two buildings. Such tendencies are accurately predicted by the simplified SPD-based method.

When PGA is 0.2g, the SRSS-based method is almost as accurate as the SPD-based method. This is because the average spectrum of 0.2G earthquakes approaches the buildings' design strength spectra, as can be imagined from Fig. 5. Thus, the buildings responded almost elastically, resulting in the small effective damping and consequently the small correlation ρ_{AB} .

Note also that, unlike the other methods, the SPD-based method implicitly includes material types and corresponding hysteretic characteristics, and it always gives very stable estimates, irrespective of any material type combinations. Although we observe some scattering of its estimates for stronger earthquakes of 0.8g PGA, the standard deviation (not shown for ABS and SRSS methods) does clearly strengthen the stable degree of the SPD-based method over the ABS- and SRSS-based methods.

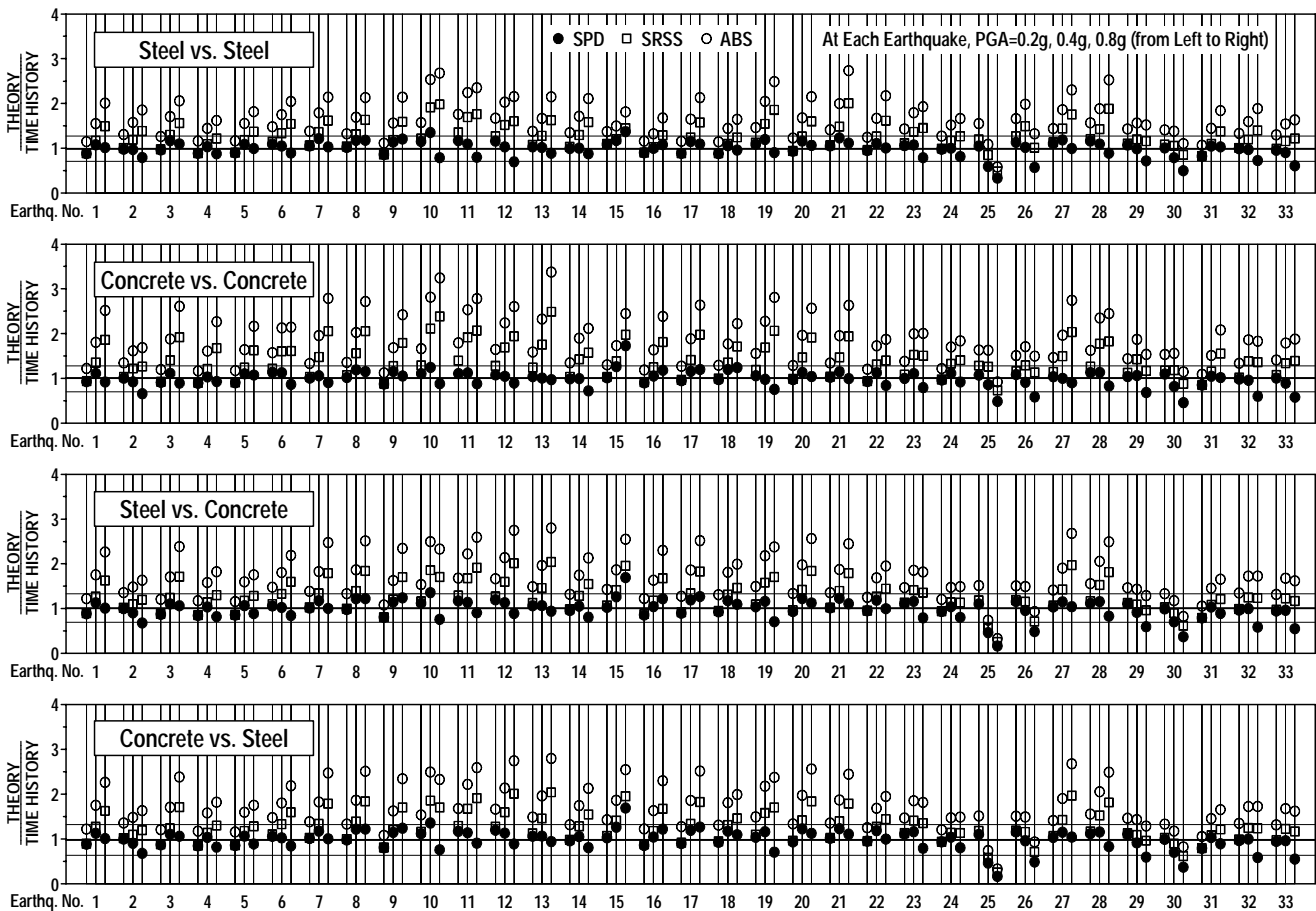


Figure 6. Average Ratios of $u_{rel}(SPD)$, $u_{rel}(SRSS)$, and $u_{rel}(ABS)$ to Exact Solution $u_{rel}(TH)$.
(Thick and thin horizontal lines represent average accuracy and average \pm standard deviation of the SPD-based method)

6. CONCLUSIONS

This paper has proposed a new method to estimate the seismic peak relative displacement between two inelastic buildings, by combining the writers' spectral difference (SPD) rule and elastic response spectrum. The conclusions are as follows:

(1) The method is validated through extensive numerical experiments using numerous code-compatible building pairs with different heights and material combinations, as well as 33 earthquakes of 2 directions, scaled to 4 different levels. The method is found to accurately estimate the relative displacement, with a narrow variability of error.

(2) Determination of relative displacement requires considerations of many factors such as; building heights, elastic vibration periods, initial yield strengths, hysteresis types, and spectrum characteristics as well as intensities of the earthquakes. Only the SPD-based method explicitly accounts for and clarifies the complex effects of these key parameters, and its use is simple.

(3) The ABS-based method is excessively conservative for the level of earthquake as well as building stiffness and strength, specified in the current code. The SRSS-based method gives a reasonably conservative estimate for moderate earthquakes, but remains incorrect for strong earthquakes because of not accounting for the relevant effect of hysteresis damping.

Acknowledgements:

The Ministry of Education, Science and Culture provided support for this study in the form of Grants-in-Aid for Scientific Research, Category C (Research Representative: Kazuhiko Kasai), and the second author's Monbu Kagakusho Scholarship. The authors gratefully acknowledge the support. The authors also thank Mr. Jagiasi for his initial participation.

References:

- Bertero, V.V. (1986), "Observation of Structural Pounding," *Proc., International Conference: the Mexico earthquake-1985*, ASCE, NY., 264-278.
- Chopra, A.K. (1995), "Dynamics of Structures: Theory and Applications to Earthquake Engineering," Prentice-Hall, Inc.
- Der Kiureghian, A. (1980), "A Response Spectrum Method For Random Vibrations," *EERC Report No. UCB/EERC-80/15*, University of California, Berkeley, California.
- IAEE (1996), "Regulations for Seismic Design, A World List – 1996," International Association for Earthq. Eng., Japan.
- IBC (2000), "International Building Code," International Code Council, Inc., Falls Church, Virginia.
- Jeng, V. and Kasai, K. (1996), "Spectral Relative Motion of Two Structures Due To Seismic Travel Waves," *J. Struct. Eng.*, ASCE, **122**(10), 1128-1135.
- Kasai, K., Ito, H., and Watanabe, A. (2003), "Peak Response Prediction for a SDOF Elasto-Plastic System Based on Equivalent Linearization Technique," *J. Struct. Constr. Eng.*, AIJ **571**(9), 53-62.
- Kasai, K., Jagiasi, R.A., and Jeng, V. (1996), "Inelastic Vibration Phase Theory For Seismic Pounding Mitigation," *J. Struct. Eng.*, ASCE, **122**(10), 1136-1147.
- Kasai, K. and Maison, B.F. (1997), "Building Pounding Damage During The 1989 Loma Prieta Earthquake," *Engineering Structures*, **19**(3), 195-207.
- Kasai, K., Motoyui, S., and Ooki, Y. (2002), "A Study on Application of Viscoelastic Dampers to a Space Frame and Response Characteristics under Horizontal Ground Motions," *J. Struct. Constr. Eng.*, AIJ **561**(11), 125-135.
- Mahin, S.A. and Lin, J. (1983), "Construction of Inelastic Response Spectra for Single Degree of Freedom Systems," *EERC Report No. UCB/EERC-83-17*, University of California, Berkeley.
- Miranda, E. (1993), "Site-Dependent Strength Reduction Factors," *J. Struct. Eng.*, ASCE, **119**(12), 3503-3519.
- Miranda E. (1994), "Evaluation of Strength Reduction Factors for Earthquake-Resistant Design," *Earthquake Spectra*, Earthquake Engineering Research Institute, **10**(2), 357-379.
- Nassar, A.A., Krawinkler, H. (1991), "Seismic Demands for SDOF and MDOF Systems," The John A. Blume Earthquake Engineering Center, Stanford University, California.
- Newmark, N.M. and Hall, W.J. (1973), "Seismic Design Criteria for Nuclear Reactor Facilities," *Report No.46*, Building Practices for Disaster Mitigation, National Bureau of Standards, U.S. Department of Commerce.
- Rosenblueth, E. and Meli, R. (1986), "The 1985 Earthquake: Causes and Effects in Mexico City," *Concrete Journal*, American Concrete Institute, **8**(5), 23-24.
- Uang, C.M. (1992), "Seismic Force Reduction and Displacement Factors," *Proceedings of 10th World Conference on Earthquake Engineering (WCEE)*, Madrid, Spain.